HHS Public Access

Author manuscript

Cell Rep. Author manuscript; available in PMC 2015 July 03.

Published in final edited form as:

Cell Rep. 2015 June 30; 11(12): 1892–1904. doi:10.1016/j.celrep.2015.05.036.

Distinct sources of hematopoietic progenitors emerge before HSCs and provide functional blood cells in the mammalian embryo

Kathleen E. McGrath[1], **Jenna M. Frame**[1], **Katherine H. Fegan**[1], **James R. Bowen**[1], **Simon J. Conway**[2], **Seana C. Catherman**[1], **Paul D. Kingsley**[1], **Anne D. Koniski**[1], and **James Palis**[1]

[1]Center for Pediatric Biomedical Research, Department of Pediatrics, University of Rochester Medical Center, Rochester, NY, USA, 14642

[2]Developmental Biology and Neonatal Medicine Program, HB Wells Center for Pediatric Research, Indiana University School of Medicine, Indianapolis, IN, USA, 46202

Summary

Hematopoietic potential arises in mammalian embryos before adult-repopulating hematopoietic stem cells (HSCs). At E9.5, we show the first murine definitive erythro-myeloid progenitors (EMPs) have an immunophenotype distinct from primitive hematopoietic progenitors, maturing megakaryocytes and macrophages, and rare B cell potential. EMPs emerge in the yolk sac with erythroid and broad myeloid, but not lymphoid, potential. EMPs migrate to the fetal liver and rapidly differentiate including production of circulating neutrophils by E11.5. While the surface markers, transcription factors and lineage potential associated with EMPs overlap with those found in adult definitive hematopoiesis, they are present in unique combinations or proportions that result in a specialized definitive embryonic progenitor. Further, we find that ES cell -derived hematopoiesis recapitulates early yolk sac hematopoiesis, including primitive, EMP and rare B cell potential. EMPs do not have long term potential when transplanted in immunocompromised adults, but can provide transient adult-like RBC reconstitution.

Introduction

Hematopoiesis in the adult consists of multipotent hematopoietic stem cells (HSCs) that differentiate through increasingly lineage-restricted progenitors that are modulated to provide a plethora of mature blood cells. However, this paradigm does not hold for the early embryo, which must simultaneously create the hematopoietic system while meeting the demands of embryonic growth and tissue differentiation with expanding blood cell numbers and lineage complexity. Additionally, hematopoietic function is required prior to the

Contact Information: James Palis at james_palis@urmc.rochester.edu.

Author Contributions

K.E.M, J.M.F, K.H.F., J.R.B., S.C.C., P.D.K. A.D.K. and J.P. performed experiments and analyzed data. S.J.C. provided founder mice for NCX1 knock-out colony. K.E.M designed experiments and wrote the manuscript with assistance from J.P. and J.M.F.

existence of HSCs in the mammalian embryo (Fujiwara et al., 1996; Kumaravelu et al., 2002; Muller et al., 1994) necessitating the emergence of alternate sources of transient hematopoietic progenitors. The first wave of embryonic hematopoiesis creates a cohort of circulating "primitive" red blood cells that mature semi-synchronously in the bloodstream and can be distinguished from later fetal and adult “definitive” erythroid cells by their large size and embryonic globin expression (Palis, 2014 for review). Primitive erythroid cells are derived from a discrete wave of extraembryonic yolk sac progenitors temporally associated with megakaryocyte and macrophage potential (Palis et al., 1999; Tober et al., 2007). However, evidence in the mouse demonstrates that primitive hematopoiesis is not sufficient to support embryonic survival until HSCs are functional (Chen et al., 2011). In the mouse embryo, there is a second wave of yolk sac-derived hematopoiesis that consists of definitive erythroid, megakaryocyte, myeloid, and multipotent progenitors (Chen et al., 2011; Palis et al., 1999, Palis, 2001). These definitive erythro-myeloid progenitors ("EMPs") are thought to be the source of the thousands of definitive erythroid progenitors and precursors found in the murine fetal liver prior to HSC colonization (Perdiguero et al., 2014; Frame et al., 2013 for review). Definitive erythroid progenitors (BFU-E) also first emerge in the yolk sac of human embryos and then are found in the fetal liver before HSCs (Frame et al., 2013 for review). In live zebrafish embryos, EMPs emerge distinct from both primitive erythropoiesis and HSCs (Bertrand et al., 2007). In the mouse, HSC-independent hematopoiesis is not only necessary, but sufficient to support the survival until birth of embryos lacking HSCs (Chen et al., 2011). Rare cells with lymphoid potential also arise before adult-transplantable HSCs, including HSC-independent B-1 cell progenitors and immature HSCs capable of becoming HSCs after ex vivo culture or when transplanted into specialized hosts (Arora et al., 2014; Kieusseian et al., 2012; Kobayashi et al., 2014; Yoder et al., 1997). However, the relationship of these cells with EMPs has not been resolved. The overlap in spatial and temporal emergence as well as shared immunophenotypic markers has hampered distinguishing the origin and contributions of these waves of embryonic hematopoiesis.

Here, we report an immunophenotype that distinguishes EMPs from maturing primitive erythroid cells, macrophages, and megakaryocytes, as well as early definitive hematopoietic progenitors with B cell or immature HSC potential. Utilizing this unique immunophenotype, EMPs were shown to emerge in the yolk sac with erythroid and broad myeloid potential, then migrate to the fetal liver and rapidly differentiate including the production of circulating neutrophils by E11.5. In adult hosts, EMP lack long-term potential, but are able to provide transient adult-like RBC reconstitution. Further, we found that ES cell-derived hematopoiesis recapitulates early yolk sac HSC-independent hematopoiesis, including distinct primitive, EMP and rare B cell potential.

Results

EMPs acquire a unique immunophenotype as they emerge in the yolk sac

The emergence of hematopoietic progenitors in the yolk sac and the AGM of the mouse embryo have been associated with kit^{+} $CD41^{+}$ cells (Ferkowicz et al., 2003; Mikkola et al., 2003; Mitjavila-Garcia et al., 2002). The E7.5 neural plate mouse conceptus contains only primitive hematopoietic progenitors (Palis et al., 1999) and lacks a distinct kit^{hi} population

(Fig. 1A). By E8.5, concurrent with the appearance of the first definitive hematopoietic colony-forming cells (CFCs), a small population of kit^{hi} CD41^{+} cells is detected in the yolk sac. A subset of E8.5 kit^{hi} CD41^{+} cells is also positive for CD16/32, an antibody that recognizes the low affinity FCγII/III receptors (Fig. 1A). Both CD16/32− positive and -negative cell fractions contain definitive hematopoietic CFC activity, as defined by definitive erythroid or granulocyte potential, which are not contained in the primitive wave of hematopoiesis (Fig. 1B, Palis et al., 1999). At E8.5, primitive erythroid CFCs were localized to the kit^{lo} CD41^{lo} population, while macrophage potential, a component of both primitive and EMP hematopoietic waves, was present in kit^{lo} and kit^{hi} populations. By E9.5, the kit^{+}CD41^{+} population increased to more than one thousand cells per yolk sac, over 90% of which are CD16/32^{+} (Fig. 1A). At E9.5, we found that the erythroid, megakaryocyte and myeloid CFCs, including high proliferative potential progenitors (HPP-CFCs), were associated with the kit^{+}CD41^{+}CD16/32^{+} population (Fig. 1C). Thus, definitive EMP potential arises at E8.25 as a kit^{hi} CD41^{+} population and by E9.5, resides in a kit^{hi} CD41^{+}CD16/32^{+} population.

E9.5 yolk sacs also contain hundreds of kit-negative cells expressing either CD41 or CD16/32 (Fig. 1D) that lack CFC potential (Fig. 1C), but express other cell surface markers consistent with maturing megakaryocytes (GP1bβ^{+} CD45$^{−}$) or macrophages (F4/80^{+} CD45^{+}), respectively (Fig. 1D). The lineage markers GP1bβ or F4/80 were not expressed on the kit^{hi} EMPs. The presence of hundreds of maturing megakaryocytes and macrophages at E9.5, when only a few EMPs are detected one day earlier, is consistent with their derivation from the hundreds of primitive hematopoietic progenitors that emerge in the yolk sac between E7.25 and E8.5. Taken together, our data indicate that by E9.5, the murine yolk sac contains several distinct populations of blood cells, which include maturing primitive erythroblasts, megakaryocytes, and macrophages, as well as an emerging population of definitive hematopoietic progenitors, EMPs, identified by their concurrent surface expression of kit, CD41 and CD16/32.

EMPs emerge in the yolk sac

Definitive hematopoietic progenitors are found in the embryo proper only after the onset of circulation (E8.25), and circulation-deficient mouse embryos lack definitive CFC in the embryo proper at E9.5 (Lux et al., 2008; Palis et al., 1999). However, other vascular beds, including the forming placenta and vitelline and umbilical vessels, have also been suggested as sites of early hematopoietic progenitor emergence (de Bruijn et al., 2000; Gordon-Keylock et al., 2013). Therefore, we reassessed the spatial and temporal emergence of EMPs in the total conceptus, using the presence of primitive erythroblasts (EryP) to estimate the contribution of yolk sac-derived blood cells found circulating in tissues (McGrath et al., 2003). At E9.5, immunophenotypic EMPs were enriched in the yolk sac, but not in the placenta or in extraembryonic vessels compared to the embryo proper (Fig. 1E). Additionally, EMPs emerged from cultured yolk sacs, but not chorion, allantois or embryo propers from pre-circulation embryos (Fig. 1F). Finally, immunophenotypic EMPs were found exclusively in the yolk sacs of E9.5 *Ncx1*-null circulation-deficient embryos (Fig. 1G). Comparable numbers of EMPs, normally distributed throughout the embryo, were concentrated in the yolk sac of *Ncx1-null* embryos (Fig. 1G). This suggests that, unlike

HSCs (North et al., 2009), EMP commitment is independent of blood flow. We conclude that EMPs emerge predominately, if not entirely, in the yolk sac.

EMP emergence is associated with markers of hemogenic endothelium and a subset of markers expressed by HSCs

HSCs co-express endothelial markers and hematopoietic markers as they emerge from hemogenic endothelium and the first definitive erythroid potential migrating into the yolk sac arises from a hemogenic endothelial precursor (Huber, 2004; Swiers et al., 2013 for review). Likewise, E9.5 kit^+ $CD41^+$ EMPs express multiple endothelial and hematopoietic markers (Fig. 1H). Unlike HSCs, EMPs express CD16/32 but not Sca1 on their cell surface (Fig. 1H) or at the transcript level (data not shown). AA4.1, a marker of fetal liver HSCs (Petrenko et al., 1999), is detected on a small proportion of E9.5 EMPs, but this may be part of EMP's endothelial marker expression. Unlike in the fetal liver, AA4.1 is expressed by E9.5 yolk sac endothelial cells (Ho et al., 2003), and the majority of $AA4.1^+$ cells in E9.5 yolk sacs are in the endothelial kit^{neg} VE-$Cadherin^+$ population (88+/− 2% of $AA4.1^+$ cells). Taken together, our data indicate that EMPs share markers of hemogenic endothelial emergence with HSCs, but can be distinguished by expression of CD16/32 and lack of Sca1 expression.

EMPs rapidly proliferate with extensive erythroid-myeloid potential

When E9.5 $kit^+CD41^+CD16/32^+$ cells were cultured in medium that supports diverse myeloid potential (Arinobu et al., 2005), they proliferated more rapidly than bone marrow hematopoietic progenitors, increasing in number approximately 10,000 fold in 6 days (Fig. 2A). This proliferation was associated with rapid maturation, as evidenced by loss of CFC activity and a large increase in hemoglobin-containing erythroid cells as well as megakaryocytes and myeloid cells visible by four days in culture (Figs. 2B and 2C). By seven days of culture, EMPs generated an extensive repertoire of cells with myeloid morphology (Fig. 2D) that expressed lineage-specific genes (Fig. 2E) including macrophages, neutrophils, basophils, eosinophils, and mast cells. Interestingly, EMPs exhibited a significantly different lineage bias compared to bone marrow progenitors, and generated more erythroid than myeloid cells. Within the myeloid lineage, EMPs also produced a higher percentage of $F4/80^+$ monocyte/macrophages, particularly large $F4/80^{hi}$ macrophages, than $GR\text{-}1^{hi}$ granulocytes (Fig. 2F, S1).

Individual EMPs can generate both erythroid and myeloid cells, as observed when E9.5 $kit^+CD41^+CD16/32^+$ cells plated in semi-solid media generated Emix colonies with erythroid and myeloid cells (Fig. 2G). Furthermore, analysis of progeny from individual EMPs in liquid culture demonstrated that 17+/−4% EMPs had both erythroid and myeloid potential (Fig. 2H, S2). EMPs express many transcription factors that regulate hematopoietic lineage decisions in adults (Iwasaki et al., 2006; Orkin and Zon, 2008) and do so at levels intermediate between adult granulocyte-monocyte progenitors (GMPs) and megakaryocyte-erythroid progenitors (MEPs), consistent with the observed erythroid and-myeloid potential of EMPs (Fig. 2I). High levels of GATA-1 and low expression of Gfi1 compared with adult GMPs also correlates with the predilection of EMPs to generate erythroblasts and macrophages.

EMPs lack B cell potential

B cell potential independent of HSC formation has been identified in the E9.5 yolk sac coincident with EMP formation (Kobayashi et al., 2014). However, EMPs lack IL7R and Flt3 cell surface markers and Pax5 transcription factor expression, which are associated with lymphoid progenitors arising from HSCs (Fig. 1H, data not shown, Adolfsson et al., 2005). Furthermore, EMPs differentiated in vitro in IL7-containing media failed to express Rag2, unlike parallel cultures of adult LK cells (Fig. 2E). Primary purified EMPs cultured on an OP9 cell monolayer generated only myeloid and erythroid cells, while $IL7R^+$ bone marrow progenitors rapidly generated $CD19^+B220^+$ cells (Fig. 3A and B). This short-term assay detects existing lymphoid progenitors, while extended cultures on OP9 stroma promotes emergence of lymphoid progenitors that then mature into B cells. As published (Yoshimoto et al., 2011), extended cultures of unfractionated E9.5 yolk sac cells differentiated at a low frequency into lymphoid progenitors by 12 days in culture (Fig. 3D), but when subfractionated B cell potential was present within the non-EMP fraction and absent in the EMP population, indicating that B cell potential emerges independently of EMPs in the E9.5 yolk sacs (Fig. 3C, D).

Differentiating embryonic stem (ES) cells recapitulate yolk sac hematopoiesis

Similar to the embryo, the first hematopoietic cells that emerge during differentiation of mouse or human ES cells are primitive erythroblasts with associated macrophages and megakaryocytes, including a primitive MEP (Fujimoto et al., 2003; Keller et al., 1993; Klimchenko et al., 2009; Paluru et al., 2014). Definitive hematopoiesis subsequently emerges, but it remains unclear whether this represents the in vitro equivalent of HSC or EMP-derived definitive potential. We found that ES cells grown as embryoid bodies (EBs) generate a population of immunophenotypic EMPs coincident with the emergence of definitive CFCs (Fig. 4B). Furthermore, definitive CFCs were predominately associated with the EMP fraction, while primitive erythroid CFCs did not reside in this population (Fig. 4C). As seen in yolk sacs, macrophage potential of EBs was associated with both primitive and EMP hematopoiesis. We next asked whether B cell potential arises independently of EMP during ES/EB differentiation by comparing EB-derived immunophenotypic EMPs with the remainder of EB cells that were additionally VE-cadherin positive (Non-EMP VEC +) to enrich for possible B cell potential in this fraction (Yoshimoto et al., 2011). As in the yolk sac, B cell potential was distinct from the sorted EMP fraction (Fig. 4D and E). Thus, initial emergence of hematopoietic potential in ES/EBs appears to recapitulate the emergence of HSC-independent yolk sac hematopoiesis, consisting of a wave of primitive hematopoiesis followed by the emergence of distinct populations of EMP-definitive progenitors and a rarer population of cells with B cell potential.

EMPs migrate to the fetal liver and differentiate including production of neutrophils

At E10.5, when the liver is colonized with hematopoietic progenitors, EMPs were found in most tissues at a similar ratio to primitive erythroid cells in the peripheral blood, indicating their widespread presence in the circulation (Fig. 5A). EMPs remained enriched in the yolk sac above peripheral blood levels, as observed at E9.5, but were more highly enriched in the liver (Fig. 1E and 5A). This distribution of immunophenotypic EMPs mirrors that of

functional CFCs in E10.5 embryos (Palis et al., 1999). Additionally, the numbers of immunophenotypic EMPs and CFC in E10.5 blood and liver are similar and day 7 CFC activity was found predominately in sorted EMP (Fig. S3). After E10.5, there is a diminution of circulating EMPs, consistent with their egress into the fetal liver, although low numbers of circulating EMPs are still detected through E14.5, suggesting they may continue to colonize the fetal liver even as HSCs expand there (Fig. 5B).

We next asked whether the extensive in vitro myeloid potential of EMPs (Fig. 3D) is realized in the embryo. Wildtype females were mated to GFP^+ males (UBC-GFP) so the resultant GFP^+ fetal blood cells could be distinguished from any contaminating GFP^- maternal cells. Rare embryonic granulocytes were detected in circulation as early as E11.5, and by E12.5, sorted GFP+ myeloid cells included those with neutrophil morphology (Figs. 5C, 5D and 5E). Myelopoiesis was evident in the fetal liver by E11.5, with megakaryocytes and macrophages comprising the majority of the non-erythroid hematopoietic cells (Fig. 5F). While these lineage ratios are consistent with the in vitro potential of EMPs, early megakaryocytes and macrophages could also derive from primitive hematopoiesis. Thus, EMP myeloid fate is best confirmed by the emergence of granulopoiesis in the murine embryo. The fetal liver contained a similar range of granulocyte intermediates, as defined by GR-1 staining and cell size, present in the bone marrow (Figs. 5G and 5H), although with higher proportion of immature forms, as expected for onset and rapid expansion of granulopoiesis (Fig. 5I). Circulating granulocytes had neutrophil morphology (Fig. 5D for example), which agrees with a lack of detectable transcripts in the early fetal liver for eosinophil peroxidase (Epx) or a shared surface marker of basophils and mast cells (FCεR) (Fig. 5J). Additionally, consistent with a neutrophil identity, a significant oxidative burst in fetal GR-1+ cells was observed after stimulation with bacterial particles (Fig. 5K). These data provide evidence that the broad granulocyte potential of EMP in vitro is refined in the early fetus to the output of functional neutrophils.

EMPs engraft adult recipients and transiently generate red blood cells with adult-like characteristics

As EMP potential temporally overlaps with that of adult repopulating HSCs or immature HSCs, (Frame et al. 2013 for review), we asked whether EMPs contain long-term hematopoietic potential using UBC-GFP mice as donors to detect of reconstitution of erythrocytes and platelets as well as myeloid and lymphoid cells (Schaefer et al., 2001). Long-term reconstitution was not found when E10.5 EMPs were transplanted into normal adult recipients or when E9.5 or E10.5 EMPs were transplanted into immunocompromised mice either by intravenous or by intrafemoral injection (Fig. 6A). In contrast, E10.5 AGM or adult bone marrow cells provided long-term multilineage reconstitution. Therefore, like early B cell potential, EMPs are independent of early HSC potential in the embryo.

EMPs did, however, provide varying degrees of short-term reconstitution (Fig. 6A). Transplanted EMPs rapidly created a wave of circulating RBCs which persisted for weeks in the adult (Fig. 6B, Fig. S4). Reconstitution was usually limited to the erythroid lineage, with only occasional small numbers of myeloid cells or platelets detected. In the fetus, EMPs generate larger RBCs that express gamma globin in embryos transgenic for the human beta-

globin locus (McGrath et al., 2011). Interestingly, in the reconstituted adult, EMP-derived RBCs were instead similar in size to adult RBCs (Fig. 6C and D). Additionally, EMPs transgenic for the human beta-globin locus generated RBCs in the adult that expressed predominately adult beta-globin (Fig. 6E). Thus, in the adult hematopoietic environment, EMPs retain their erythroid-biased short-term hematopoietic potential but generate mature erythrocytes with adult, rather than fetal, characteristics.

Discussion

The first blood cells in mammalian embryos consist of large nucleated "primitive" erythroid cells that arise from a transient wave of yolk sac progenitors. They are replaced in the fetus by smaller, enucleated red cells that were termed "definitive" more than a century ago (Maximov, 1909). Fetal and postnatal definitive RBCs were assumed to comprise one continuous lineage derived from HSCs. While there is clear evidence that this two-wave model is an oversimplification, the legacy of this model and its nomenclature still influences many interpretations of hematopoietic emergence. Primitive hematopoiesis is not restricted to erythroid cells, but is associated with macrophage and megakaryocyte potential (Palis et al., 1999; Paluru et al., 2014; Tober et al., 2007; Hoeffel et al. 2015). Our data have shown further that primitive and EMP-associated macrophage progenitors can be distinguished prospectively by immunophenotype. Consistent with a tri-lineage primitive hematopoietic potential, we and others have identified populations of maturing macrophages and megakaryocytes in the E9.5 yolk sac prior to formation of the fetal liver (Tober et al. 2007; Perdiguero et al. 2014; Hoeffel et al. 2015). The expression of CD41 and CD45 on these cells complicates the use of these markers in the identification of co-emerging definitive hematopoietic progenitors.

It has also become clear that along with the primitive hematopoietic potential, definitive blood cells also arise independently of HSC. In both human and mouse embryos, the first definitive erythroid progenitors emerge in the yolk sac before HSC arise and colonize the fetal liver prior to HSC (Frame et al. 2013 for review). While kit and CD41 mark both EMP and HSC emergence (Bertrand et al., 2005; Ferkowicz et al., 2003; Mikkola et al., 2003; Mitjavila-Garcia et al., 2002), we find that EMPs also become CD16/32^{+}, a triple-positive immunophenotype without corollary in the adult hematopoietic hierarchy (Miyawaki et al., 2014; Pronk et al., 2007). This phenotype made it possible to trace EMP emergence in the E8.5-9.5 yolk sac and their colonization of the fetal liver at E10.5-11.5. In contrast to the small numbers of adult transplantable and/or immature HSCs detected per embryo until E12.5, thousands of EMPs and hundreds of thousands of hematopoietic intermediates are detected during this time. These data complement lineage tracing experiments demonstrating yolk sac progenitors contribute significantly to fetal liver myelopoiesis (Perdiguero et al. 2014; Hoeffel et al. 2015). While mouse embryos defective in HSC formation survive until birth, embryos with defects in primitive erythropoiesis die as early as E9.5, and those with defects in EMP-derived definitive erythropoiesis die by E15.5 (Chen et al., 2011; Fujiwara et al., 1996; Mucenski et al., 1991). Thus, the yolk sac provides erythroid and myeloid function through two distinct waves of progenitors that sequentially support embryogenesis until HSC-derived hematopoiesis is established at later stages of gestation.

EMPs generate erythroid cells, megakaryocytes and a wide range of myeloid lineages in vitro. Our clonal analyses confirmed the presence of single EMPs with erythroid and myeloid potential, consistent with "common myeloid progenitors" (CMPs). However, there are important distinctions between EMPs and adult CMPs. In the adult, CD16/32 is expressed at low levels in CMPs and high levels in GMPs, which have lost erythroid and megakaryocyte potential (Akashi et al., 2000). Furthermore, adult murine CMPs can be subfractionated into a $CD150^{+}$ population with mainly MEP potential and a $CD150^{-}$ population with mainly GMP potential (Pronk et al., 2007). In contrast, EMPs express high levels of CD16/32 and lack CD150 expression, yet are still strongly biased to generate erythroid cells and megakaryocytes. In vitro, EMPs are also biased to produce more macrophages than granulocytes, while CMPs preferentially form granulocytes (Akashi et al., 2000). These in vitro lineage biases are consistent with their expression profile of transcription factors known to control adult erythro-myeloid lineage choice. This suggests that EMPs not only make definitive, or adult-like, blood cells, but may share transcriptional regulators with adult hematopoiesis in altered proportions that generate a hematopoietic progenitor specifically designed to meet the needs of the rapidly growing embryo.

Primitive hematopoietic progenitors and EMPs each generate megakaryocytes and macrophages. It has recently been demonstrated that yolk sac progenitors are an important source of multiple tissue-resident macrophages in the adult. Both primitive and EMP-derived macrophages have been traced to different adult tissues. (Kierdorf et al., 2013; Perdiguero et al., 2014; Schulz et al., 2012; Ginhoux et al. 2010; Hoeffel et al. 2015). The first definitive erythroid and granulocyte potential in the mouse embryo are derived from EMPs and not from primitive hematopoiesis, and thus we used these lineages to specifically analyze EMP differentiation. Our previous studies demonstrated expanding definitive erythropoiesis in the fetal liver and the first definitive erythrocytes in the circulation by E11.5 (McGrath et al., 2011). Similarly, we report here that fetal granulocytes are present in the liver and bloodstream by E11.5 and then expand rapidly in both compartments. Interestingly, the wider granulocytic potential of EMPs is apparently narrowed to a neutrophil fate in the early fetus. Although we do not yet know if neutrophils have a role in mammalian embryogenesis, fetal neutrophils exhibited antibacterial oxidation responses consistent with a role in host defense. There are also possible roles for neutrophils in angiogenesis and niche interactions as seen in the adult (Casanova-Acebes et al., 2014; Christoffersson et al., 2012).

The emergence of lymphoid or long-term hematopoietic potential temporally overlaps with EMP emergence (Godin et al., 1995; Kieusseian et al., 2012; Kumaravelu et al., 2002; Yoder et al., 1997; Yoshimoto et al., 2011; Yoshimoto et al., 2012). While it is unclear how these latter potentials relate to one another, they have characteristics distinct from EMPs. Both lymphoid and nascent HSC emergences are more broadly distributed and considerably more rare than EMPs. However, the overlap in markers and timing could indicate they comprise a subset of EMPs. Our analysis of purified populations of EMPs demonstrated that early lymphoid and HSC potential are indeed distinct at E9.5. Taken together, these data indicate that the emergence of hematopoiesis in the embryo is remarkably complex, with distinct hematopoietic populations that have varied spatio-temporal emergence, abundance, lineage potential and persistence. It is important to note that our studies have focused on the

onset of hematopoiesis and prior to significant HSC expansion, so they do not rule out the possibility that hematopoietic progenitors continue to evolve in their phenotype or potential over time.

Ultimately, it will be important to determine how hematopoietic stem and progenitor cells with different lineage restrictions and self-renewal potential are generated in the developing embryo. ES and iPS cells are important experimental models of hematopoietic emergence with the promise of serving as a source of cell-based therapies. However, the absence of precise temporal and spatial cues makes it difficult to correlate findings in the ES/iPS system with those known to occur in the embryo. By comparing our observations in the embryo directly with those from differentiating ES cells, we found that ES cells recapitulated the hematopoietic development present in the yolk sac, including primitive hematopoietic, definitive EMP and rare B cell potential. This is not unexpected, given that these models mimic early embryogenesis and hematopoiesis generated from yolk sac progenitors account for almost all of the blood cells seen in the murine embryo from E7.5 to E12.5. The ability to identify and track yolk sac-derived hematopoietic lineages should facilitate future studies directing the development of ES/iPS cell systems beyond the yolk sac phase of hematopoietic emergence toward the formation of HSCs. Additionally, given their potential to provide short-term definitive erythrocytes, platelets and granulocytes, EMPs might also serve therapeutic roles. A better understanding of EMP will be critical to increase the cellular output and compatibility with the adult hematopoietic microenvironment.

Experimental Procedures

Mice, Tissue Collection and Processing

Mice were used in accordance with the guidelines of the University of Rochester School of Medicine and Dentistry Institutional Animal Care and Use Committee. Mice were maintained on 12-hour dark and light cycles. See supplemental experimental information for strains used. Mice were mated overnight and vaginal plugs examined in the morning (E0.3). Mice were sacrificed by CO_2 narcosis. Embryonic tissues were isolated from staged embryos and dissociated as previously described (McGrath et al., 2011). Adult peripheral blood was collected from a tail or submandibular vein for analysis of reconstitution or was collected from the descending vena cava for terminal analysis. Femoral marrow was flushed and dissociated by trituration. For transplantation, cells were either injected in the tail vein or intrafemorally (Schmitz et al., 2011) into recipients pre-conditioned with 5Gy TBI for C57B6 and 1.5Gy TBI for NSG mice.

In Vitro Cultures

Colony forming assays for megakaryocyte progenitors, erythroid and myeloid progenitors and high proliferative potential progenitors were performed as previously described (Palis et al., 2001; Palis and Koniski, 2005). Embryonic tissues were explanted with two embryo equivalents in 100 ul of media as described (Shah et al., 2013). Sorted cells were cultured in maturation media (Arinobu et al., 2005) containing 20 ng/ml murine stem cell factor, IL-3, IL-6, and IL-7; 50 ng/ml IL-5 and IL-9; 10 ng/ml IL-11, granulocyte-macrophage colony-

stimulating factor and thrombopoietin, (all Peprotech), and 2 U/ml erythropoietin (Amgen) at 10^5cells/ml or less. Short-term and long-term assays of B cell progenitors were performed as described (Yoshimoto et al., 2011).

ES/EB cells

PC13 embryonic stem cells (University of Rochester Transgenic Facility) and W4 cell lines (developed in the laboratory of Dr. Alex Joyner at NYU School of medicine) were cultured as EBs essentially as described (England et al., 2011) except that EBs were dissociated using collagenase type 1 according to manufacturer's instructions (Stemcell Technologies).

Cell staining and microscopy

Cytospun cells were stained using an automated Wright stain (Sigma) as described (Kingsley et al., 2004) or stained with standard Hematoxylin and Eosin (H&E) or acetylcholinesterase (ACE). Photomicroscopy was performed on a Nikon Eclipse 80i microscope using a 100X objective or for colonies a Nikon TE2000 and a 20x objective. Images were captured with a Nikon DS-Fi1 camera and minimally processed using Nikon Elements AR or Photoshop software.

PCR

For RT-PCR, RNA was extracted using RNeasy Plus Mini Kits (Qiagen), and cDNA synthesized utilizing SuperScript First-Strand Synthesis Systems (Invitrogen) according to manufacture's instructions. For quantitative RT-PCR, cDNA was made from sorted cells using the Cells to CT kit according to manufacturer's instructions (ABI). Primers and conditions are contained in supplemental experimental information. Expression levels were normalized to 18S transcript levels.

Flow Cytometry and Cell Sorting

Cells were blocked with 10% normal rat serum (Invitrogen) and then stained as indicated in experimental supplementary information with 1:100 dilutions of antibodies, vital DNA stain (10 uM DRAQ5 (eBioscience), or Vibrant Violet as recommended (Invitrogen) and live/dead discriminator (1 ug/ml propidium iodide or 5 ug/ml DAPI: Invitrogen). Engraftment of RBC and platelets was assayed using 2 ul of whole blood and engraftment of myeloid cells was determined using 50 ul of blood analyzed after RBC lysis. Oxidative burst assay was performed after stimulation of cells with S. aureus bioparticles (Lifetechnologies) and detected utilizing dihydroethidium (DHE: Sigma) as reported (McFarlin et al., 2013). Cells were sorted using a FACS Aria or analyzed on an LSRII (BD Bioscience) using FlowJo analysis software (Treestar). Imaging flow cytometric data were collected on a ImageStreamX and analyzed using IDEAS 6.0 (Amnis).

Supplementary Material

Refer to Web version on PubMed Central for supplementary material.

Acknowledgements

The authors thank Leah Vit for technical assistance, the Flow Cytometry Core Facility at the University of Rochester Medical Center for technical support, Dr. Momoko Yoshimoto for assistance with B-lymphoid assays and Dr. Kenneth R. Peterson for providing transgenic mice with the human beta globin locus. This study was supported by funds from the Michael Napoleone Memorial Foundation and the NIH/NIDDK (R01 DK079361 to J.P.)

References

Adolfsson J, Mansson R, Buza-Vidas N, Hultquist A, Liuba K, Jensen CT, Bryder D, Yang L, Borge OJ, Thoren LA, et al. Identification of Flt3+ lympho-myeloid stem cells lacking erythro-megakaryocytic potential a revised road map for adult blood lineage commitment. Cell. 2005; 121:295–306. [PubMed: 15851035]

Akashi K, Traver D, Miyamoto T, Weissman IL. A clonogenic common myeloid progenitor that gives rise to all myeloid lineages. Nature. 2000; 404:193–197. [PubMed: 10724173]

Arinobu Y, Iwasaki H, Gurish MF, Mizuno S, Shigematsu H, Ozawa H, Tenen DG, Austen KF, Akashi K. Developmental checkpoints of the basophil/mast cell lineages in adult murine hematopoiesis. Proc Natl Acad Sci U S A. 2005; 102:18105–18110. [PubMed: 16330751]

Arora N, Wenzel PL, McKinney-Freeman SL, Ross SJ, Kim PG, Chou SS, Yoshimoto M, Yoder MC, Daley GQ. Effect of developmental stage of HSC and recipient on transplant outcomes. Dev Cell. 2014; 29:621–628. [PubMed: 24914562]

Bertrand JY, Giroux S, Golub R, Klaine M, Jalil A, Boucontet L, Godin I, Cumano A. Characterization of purified intraembryonic hematopoietic stem cells as a tool to define their site of origin. Proc Natl Acad Sci U S A. 2005; 102:134–139. [PubMed: 15623562]

Bertrand JY, Kim AD, Violette EP, Stachura DL, Cisson JL, Traver D. Definitive hematopoiesis initiates through a committed erythromyeloid progenitor in the zebrafish embryo. Development. 2007; 134:4147–4156. [PubMed: 17959717]

Casanova-Acebes M, N AG, Weiss LA, Hidalgo A. Innate immune cells as homeostatic regulators of the hematopoietic niche. Int J Hematol. 2014; 99:685–694. [PubMed: 24634109]

Chen MJ, Li Y, De Obaldia ME, Yang Q, Yzaguirre AD, Yamada-Inagawa T, Vink CS, Bhandoola A, Dzierzak E, Speck NA. Erythroid/myeloid progenitors and hematopoietic stem cells originate from distinct populations of endothelial cells. Cell Stem Cell. 2011; 9:541–552. [PubMed: 22136929]

Christoffersson G, Vagesjo E, Vandooren J, Liden M, Massena S, Reinert RB, Brissova M, Powers AC, Opdenakker G, Phillipson M. VEGF-A recruits a proangiogenic MMP-9-delivering neutrophil subset that induces angiogenesis in transplanted hypoxic tissue. Blood. 2012; 120:4653–4662. [PubMed: 22966168]

de Bruijn MF, Speck NA, Peeters MC, Dzierzak E. Definitive hematopoietic stem cells first develop within the major arterial regions of the mouse embryo. EMBO J. 2000; 19:2465–2474. [PubMed: 10835345]

England SJ, McGrath KE, Frame JM, Palis J. Immature erythroblasts with extensive ex vivo self-renewal capacity emerge from the early mammalian fetus. Blood. 2011; 117:2708–2717. [PubMed: 21127173]

Ferkowicz MJ, Starr M, Xie X, Li W, Johnson SA, Shelley WC, Morrison PR, Yoder MC. CD41 expression defines the onset of primitive and definitive hematopoiesis in the murine embryo. Development. 2003; 130:4393–4403. [PubMed: 12900455]

Frame JM, McGrath KE, Palis J. Erythro-myeloid progenitors: "definitive" hematopoiesis in the conceptus prior to the emergence of hematopoietic stem cells. Blood Cells Mol Dis. 2013; 51:220–225. [PubMed: 24095199]

Fujimoto TT, Kohata S, Suzuki H, Miyazaki H, Fujimura K. Production of functional platelets by differentiated embryonic stem (ES) cells in vitro. Blood. 2003; 102:4044–4051. [PubMed: 12920021]

Fujiwara Y, Browne CP, Cunniff K, Goff SC, Orkin SH. Arrested development of embryonic red cell precursors in mouse embryos lacking transcription factor GATA-1. Proc Natl Acad Sci U S A. 1996; 93:12355–12358. [PubMed: 8901585]

Ginhoux F, Greter M, Leboeuf M, Nandi S, See P, Gokhan S, Mehler MF, Conway SJ, Ng LG, Stanley ER, et al. Fate mapping analysis reveals that adult microglia derive from primitive macrophages. Science. 2010; 330:841–845. [PubMed: 20966214]

Godin I, Dieterlen-Lièvre F, Cumano A. Emergence of multipotent hemopoietic cells in the yolk sac and paraaortic splanchnopleura in mouse embryos, beginning at 8.5 days postcoitus. Proc Natl Acad Sci U S A. 1995; 92:773–777. [PubMed: 7846049]

Gordon-Keylock S, Sobiesiak M, Rybtsov S, Moore K, Medvinsky A. Mouse extra-embryonic arterial vessels harbor precursors capable of maturing into definitive HSCs. Blood. 2013

Ho M, Yang E, Matcuk G, Deng D, Sampas N, Tsalenko A, Tabibiazar R, Zhang Y, Chen M, Talbi S, et al. Identification of endothelial cell genes by combined database mining and microarray analysis. Physiol Genom. 2003; 13:249–262.

Hoeffel G, Chen J, Lavin Y, Low D, Almeida FF, See P, Beaudin AE, Lum J, Low I, Forsberg EC, et al. C-myb(+) erythro-myeloid progenitor-derived fetal monocytes give rise to adult tissue-resident macrophages. Immunity. 2015; 42:665–678. [PubMed: 25902481]

Huber TL, Kouskoff V, Fehling HJ, Palis J, Keller G. Haemangioblast commitment is initiated in the primitive streak of the mouse embryo. Nature. 2004; 432:625–630. [PubMed: 15577911]

Iwasaki H, Mizuno S, Arinobu Y, Ozawa H, Mori Y, Shigematsu H, Takatsu K, Tenen DG, Akashi K. The order of expression of transcription factors directs hierarchical specification of hematopoietic lineages. Genes Dev. 2006; 20:3010–3021. [PubMed: 17079688]

Keller G, Kennedy M, Papayannopoulou T, Wiles MV. Hematopoietic commitment during embryonic stem cell differentiation in culture. Mol Cell Biol. 1993; 13:473–486. [PubMed: 8417345]

Kierdorf K, Erny D, Goldmann T, Sander V, Schulz C, Perdiguero EG, Wieghofer P, Heinrich A, Riemke P, Holscher C, et al. Microglia emerge from erythromyeloid precursors via Pu.1- and Irf8-dependent pathways. Nat Neurosci. 2013; 16:273–280. [PubMed: 23334579]

Kieusseian A, Brunet de la Grange P, Burlen-Defranoux O, Godin I, Cumano A. Immature hematopoietic stem cells undergo maturation in the fetal liver. Development. 2012; 139:3521–3530. [PubMed: 22899849]

Kingsley PD, Malik J, Fantauzzo KA, Palis J. Yolk sac-derived primitive erythroblasts enucleate during mammalian embryogenesis. Blood. 2004; 104:19–25. [PubMed: 15031208]

Klimchenko O, Mori M, Distefano A, Langlois T, Larbret F, Lecluse Y, Feraud O, Vainchenker W, Norol F, Debili N. A common bipotent progenitor generates the erythroid and megakaryocyte lineages in embryonic stem cell-derived primitive hematopoiesis. Blood. 2009; 114:1506–1517. [PubMed: 19478046]

Kobayashi M, Shelley WC, Seo W, Vemula S, Lin Y, Liu Y, Kapur R, Taniuchi I, Yoshimoto M. Functional B-1 progenitor cells are present in the hematopoietic stem cell-deficient embryo and depend on Cbfbeta for their development. Proc Natl Acad Sci U S A. 2014; 111:12151–12156. [PubMed: 25092306]

Kumaravelu P, Hook L, Morrison AM, Ure J, Zhao S, Zuyev S, Ansell J, Medvinsky A. Quantitative developmental anatomy of definitive haematopoietic stem cells/long-term repopulating units (HSC/RUs): role of the aorta-gonad-mesonephros (AGM) region and the yolk sac in colonisation of the mouse embryonic liver. Development. 2002; 129:4891–4899. [PubMed: 12397098]

Lux CT, Yoshimoto M, McGrath K, Conway SJ, Palis J, Yoder MC. All primitive and definitive hematopoietic progenitor cells emerging before E10 in the mouse embryo are products of the yolk sac. Blood. 2008; 111:3435–3438. [PubMed: 17932251]

Maximov A. Untersuchungen uber blut und bindegewebe 1. Die fruhesten entwicklungsstadien der blut- und binde-gewebszellan bein saugetierembryo, bis zum anfang der blutbilding unden leber. Arch Mikrosk Anat. 1909; 73:444–561.

McFarlin BK, Williams RR, Venable AS, Dwyer KC, Haviland DL. Image-based cytometry reveals three distinct subsets of activated granulocytes based on phagocytosis and oxidative burst. Cytometry A. 2013; 83:745–751. [PubMed: 23839911]

McGrath KE, Frame JM, Fromm GJ, Koniski AD, Kingsley PD, Little J, Bulger M, Palis J. A transient definitive erythroid lineage with unique regulation of the beta-globin locus in the mammalian embryo. Blood. 2011; 117:4600–4608. [PubMed: 21378272]

McGrath KE, Koniski AD, Malik J, Palis J. Circulation is established in a stepwise pattern in the mammalian embryo. Blood. 2003; 101:1669–1676. [PubMed: 12406884]

Mikkola HK, Fujiwara Y, Schlaeger TM, Traver D, Orkin SH. Expression of CD41 marks the initiation of definitive hematopoiesis in the mouse embryo. Blood. 2003; 101:508–516. [PubMed: 12393529]

Mitjavila-Garcia MT, Cailleret M, Godin I, Nogueira MM, Cohen-Solal K, Schiavon V, Lecluse Y, Le Pesteur F, Lagrue AH, Vainchenker W. Expression of CD41 on hematopoietic progenitors derived from embryonic hematopoietic cells. Development. 2002; 129:2003–2013. [PubMed: 11934866]

Miyawaki K, Arinobu Y, Iwasaki H, Kohno K, Tsuzuki H, Iino T, Shima T, Kikushige Y, Takenaka K, Miyamoto T, et al. CD41 marks the initial myelo-erythroid lineage specification in adult mouse hematopoiesis: Redefinition of murine common myeloid progenitor. Stem Cells. Nov 29.2014 doi: 10.1002/stem.1906.

Mucenski ML, McLain K, Kier AB, Swerdlow SH, Schreiner CM, Miller TA, Pietryga DW, Scott WJ Jr. Potter SS. A functional c-myb gene is required for normal murine fetal hepatic hematopoiesis. Cell. 1991; 65:677–689. [PubMed: 1709592]

Muller AM, Medvinsky A, Strouboulis J, Grosveld F, Dzierzak E. Development of hematopoietic stem cell activity in the mouse embryo. Immunity. 1994; 1:291–301. [PubMed: 7889417]

North TE, Goessling W, Peeters M, Li P, Ceol C, Lord AM, Weber GJ, Harris J, Cutting CC, Huang P, et al. Hematopoietic stem cell development is dependent on blood flow. Cell. 2009; 137:736–748. [PubMed: 19450519]

Orkin SH, Zon LI. Hematopoiesis: an evolving paradigm for stem cell biology. Cell. 2008; 132:631–644. [PubMed: 18295580]

Palis J. Primitive and definitive erythropoiesis in mammals. Front Physiol. 2014; 5:3. [PubMed: 24478716]

Palis J, Chan RJ, Koniski A, Patel R, Starr M, Yoder MC. Spatial and temporal emergence of high proliferative potential hematopoietic precursors during murine embryogenesis. Proc Natl Acad Sci U S A. 2001; 98:4528–4533. [PubMed: 11296291]

Palis J, Koniski A. Analysis of hematopoietic progenitors in the mouse embryo. Methods in molecular medicine. 2005; 105:289–302. [PubMed: 15492402]

Palis J, Robertson S, Kennedy M, Wall C, Keller G. Development of erythroid and myeloid progenitors in the yolk sac and embryo proper of the mouse. Development. 1999; 126:5073–5084. [PubMed: 10529424]

Paluru P, Hudock KM, Cheng X, Mills JA, Ying L, Galvão AM, Lu L, Tiyaboonchai A, Sim X, Sullivan SK, et al. The negative impact of Wnt signaling on megakaryocyte and primitive erythroid progenitors derived from human embryonic stem cells. Stem Cell Res. 2014; 12:441–451. [PubMed: 24412757]

Perdiguero EG, Klapproth K, Schulz C, Busch K, Azzoni E, Crozet L, Garner H, Trouillet C, de Bruijn MF, Geissmann F, et al. Tissue-resident macrophages originate from yolk-sac-derived erythro-myeloid progenitors. Nature. 2014

Petrenko O, Beavis A, Klaine M, Kittappa R, Godin I, Lemischka IR. The Molecular Characterization of the Fetal Stem Cell Marker AA4. Immunity. 1999; 10:691–700. [PubMed: 10403644]

Pronk CJ, Rossi DJ, Mansson R, Attema JL, Norddahl GL, Chan CK, Sigvardsson M, Weissman IL, Bryder D. Elucidation of the phenotypic, functional, and molecular topography of a myeloerythroid progenitor cell hierarchy. Cell Stem Cell. 2007; 1:428–442. [PubMed: 18371379]

Schaefer BC, Schaefer ML, Kappler JW, Marrack P, Kedl RM. Observation of antigen-dependent CD8+ T-cell/ dendritic cell interactions in vivo. Cell Immunol. 2001; 214:110–122. [PubMed: 12088410]

Schmitz M, Bourquin JP, Bornhauser BC. Alternative technique for intrafemoral injection and bone marrow sampling in mouse transplant models. Leuk Lymphoma. 2011; 52:1806–1808. [PubMed: 21663514]

Schulz C, Gomez Perdiguero E, Chorro L, Szabo-Rogers H, Cagnard N, Kierdorf K, Prinz M, Wu B, Jacobsen SE, Pollard JW, et al. A lineage of myeloid cells independent of Myb and hematopoietic stem cells. Science. 2012; 336:86–90. [PubMed: 22442384]

Shah RR, Koniski A, Shinde M, Blythe SA, Fass DM, Haggarty SJ, Palis J, Klein PS. Regulation of primitive hematopoiesis by class I histone deacetylases. Dev Dyn. 2013; 242:108–121. [PubMed: 23184530]

Swiers G, Rode C, Azzoni E, de Bruijn MFTR. A short history of hemogenic endothelium. Blood Cells Mol Dis. 2013; 51:206–212. [PubMed: 24095001]

Tober J, Koniski A, McGrath KE, Vemishetti R, Emerson R, de Mesy-Bentley KK, Waugh R, Palis J. The megakaryocyte lineage originates from hemangioblast precursors and is an integral component both of primitive and of definitive hematopoiesis. Blood. 2007; 109:1433–1441. [PubMed: 17062726]

Yoder MC, Hiatt K, Dutt P, Mukherjee P, Bodine DM, Orlic D. Charactorization of definitive lymphomematopoietic stem cells in the day 9 murine yolk sac. Immunity. 1997; 7:335–344. [PubMed: 9324354]

Yoshimoto M, Montecino-Rodriguez E, Ferkowicz MJ, Porayette P, Shelley WC, Conway SJ, Dorshkind K, Yoder MC. Embryonic day 9 yolk sac and intra-embryonic hemogenic endothelium independently generate a B-1 and marginal zone progenitor lacking B-2 potential. Proc Natl Acad Sci U S A. 2011; 108:1468–1473. [PubMed: 21209332]

Yoshimoto M, Porayette P, Glosson NL, Conway SJ, Carlesso N, Cardoso AA, Kaplan MH, Yoder MC. Autonomous murine T-cell progenitor production in the extra-embryonic yolk sac before HSC emergence. Blood. 2012; 119:5706–5714. [PubMed: 22431573]

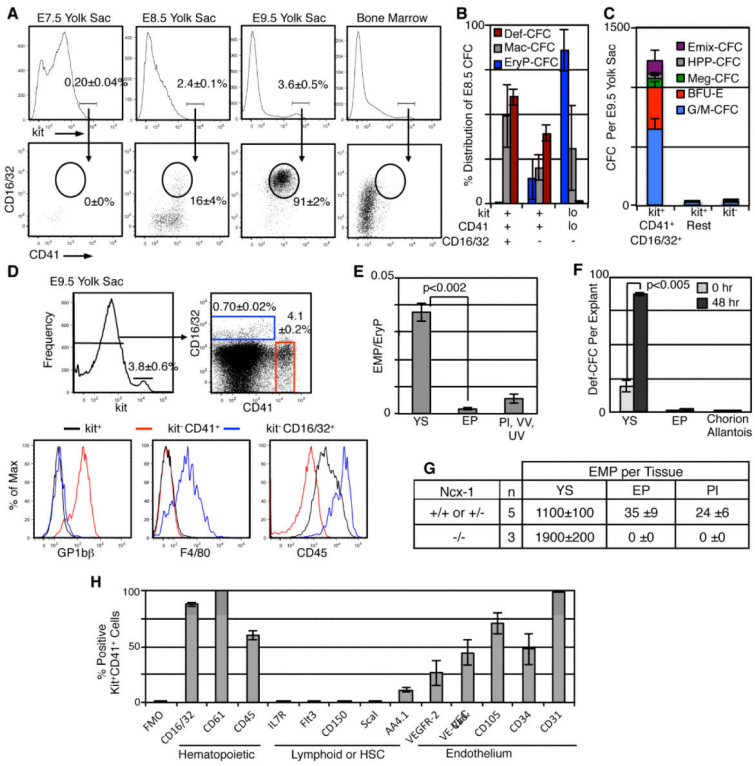

Figure 1.

EMPs acquire a distinct cell surface phenotype as they emerge in the yolk sac. **A.** Analysis of yolk sac or bone marrow cells for expression of kit, CD41 and CD16/32. **B.** Distribution of CFCs in sorted E8.5 yolk sac cells. Def-CFCs represent the sum of colonies containing definitive erythroid cells and/or granulocytes (BFU-E, CFC-G, CFC-GM, or Emix). **C.** Hematopoietic potential of E9.5 yolk sac populations. **D.** Expression of megakaryocyte or macrophage surface markers on E9.5 yolk sac cells. Kit^{+}(black), $kit^{-}CD16/32^{+}$ (blue), $kit^{-}CD41^{+}$ (red) populations (top graphs) were examined for maturation markers (bottom graphs). One example of three experiments with similar results is shown. **E**. Ratio of immunophenotypic EMPs versus circulating primitive erythroblasts in dissected E9.5 conceptus. YS=yolk sac, EP= embryo proper, Pl= Placenta, VV and UV= viteline and umbilical vessels. **F.** Increases in definitive CFC in explanted E8.5 tissues after 48 hours. **G.** Numbers of immunophenotypic EMPs in Ncx1-null versus heterozygotes or wildtype E9.5 tissues. **H.** Immunophenotype of kit^{+} $CD41^{+}$ E9.5 yolk sac cells. Gating of positive cells was determined using a fluorescence minus one plus isotype negative control (FMO). In all graphs the average of 3 to 5 experiments is plotted +/− SEM.

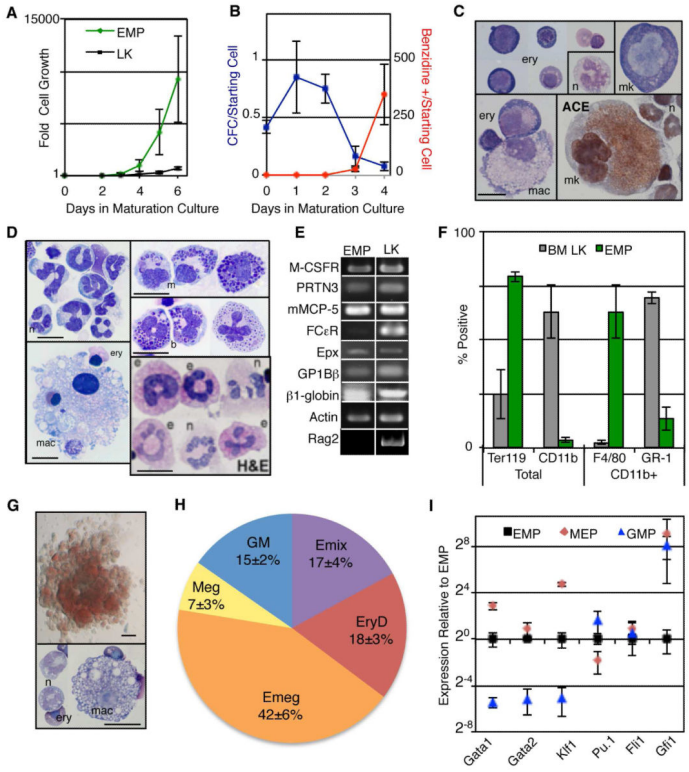

Figure 2.

EMPs are multipotential progenitors that rapidly proliferate and differentiate into a wide variety of erythroid-myeloid cells. **A.** Increases in cell numbers relative to starting numbers in cultures of sorted EMPs or adult lineage negative kit$^+$ cells (LKs). **B.** Loss of colony forming ability and accumulation of benzidine positive cells in the first 4 days of EMP culture. **C.** Morphology of cytospun cells generated by day 4 of maturation cultures of EMPs showing maturing erythroblasts (ery), megakaryocytes (mk), macrophages (m) and occasional neutrophils (n). Cells were stained with Wright's stain acetylcholinesterase (ACE) staining (bottom right) for megakaryocytes, size bar=25 um. **D.** Morphology of EMP progeny after 7 days. Cytospun cells stained with Wrights stain or H&E (bottom right). Size bar is 25 um. n=neutrophil, m=mast, b= basophil, e=eosinophil, mac= macrophage, ery=erythroblast. **E.** Erythroid, myeloid and lymphoid gene expression detected by RT-PCR in 7 day EMP and LK cultures. Genes expressed in macrophages (M-CSFR) neutrophils (PRTN3), mast cells (mMCP-5,FCεR), basophils (FCεR), megakaryocytes (GP1Bβ), erythroblasts (β1-globin) and lymphoid cells (Rag2) are shown. Representative example of three experiments is shown. **F.** Flow cytometric analysis of cells produced at day 6 of EMP and LK cultures with lineage specific markers comparing proportions of erythroid (Ter119$^+$) versus myeloid (CD11b$^+$) and monocyte/macrophage (F4/80$^+$) versus granulocyte (GR-1$^+$) within the CD11b$^+$ fraction. Example of gated populations in Fig. S1. Average of 3 to 5 experiments +/− SEM. The difference between percent EMP versus LK derived cells in each fraction was significant ($p<0.001$). **G.** E9.5 EMP-derived Emix colony and the cytospun cells within it (below) Size bars: top=200 um, bottom=25 um. **H.** Lineage combinations present after 6 days of liquid culture of individual E9.5 EMPs. Wells with robust growth (ranging from 10 to 20% of total wells) were analyzed by flow cytometry (see SI Fig. 1B).

All experiments were repeated 3 to 5 times to obtain the average +/− SEM. **I.** qPCR of transcription factor expression in sorted adult GMPs and MEPs normalized to levels found in sorted EMPs.

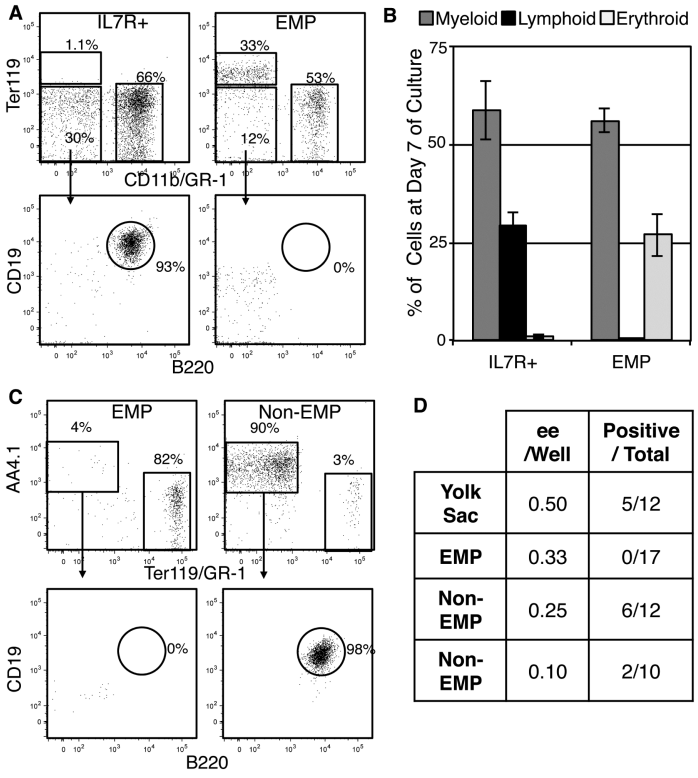

	ee /Well	Positive / Total
Yolk Sac	0.50	5/12
EMP	0.33	0/17
Non-EMP	0.25	6/12
Non-EMP	0.10	2/10

Figure 3.

E9.5 yolk sac B lymphoid potential is not derived from EMPs. **A.** Sorted E9.5 EMPs or bone marrow IL7R^{+} cells were cultured for 7 days on OP9 stroma and examined by flow cytometry for erythroid (Ter119^{+}) myeloid (CD11b or GR-1^{+}) or B lymphoid (B220^{+}CD19^{+}) markers. **B.** Quantitation of experiments in A. n=3 +/− SEM **C.** Potential to differentiate into B cell progenitors was examined in OP9 stromal co-culture with removal of non-adherent cells at 5 and 7 days and analysis at day 10 and 12 for B cells (AA4.1^{+} CD19^{+} B220^{+}). **D.** Frequency of cultures that generated lymphoid progenitors after 12 days. Dissociated total yolk sac cells or cells with EMP immunophenotype or the remainder (Non-EMP) were used. ee=embryo equivalent.

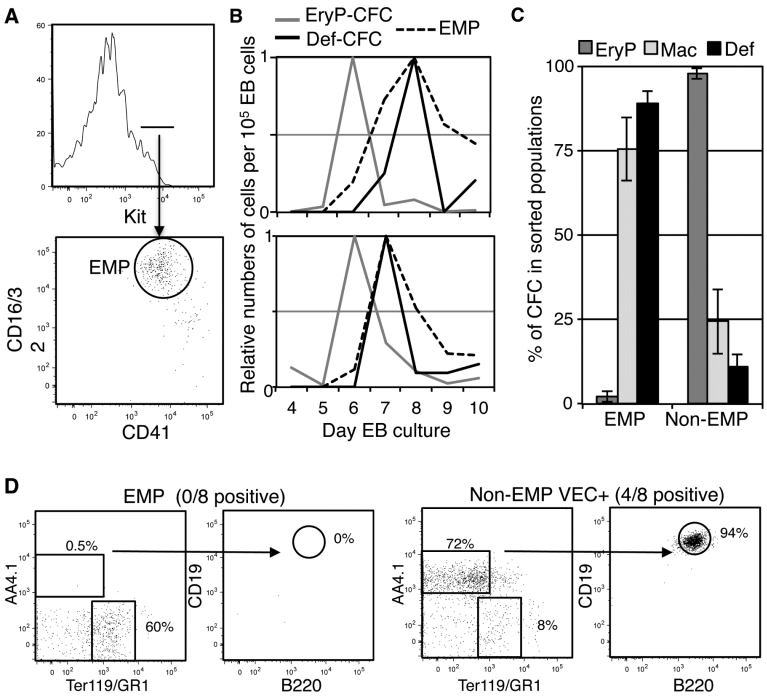

Figure 4.

Differentiation of ES cells generates temporal waves of hematopoiesis similar to the yolk sac. **A.** Emergence of a kit$^+$CD41$^+$CD16/32$^+$ population during differentiation of ES cells as embryoid bodies (EBs). Example of day 8 EB from W4 ES cell line is shown. **B.** Representative examples of waves of definitive CFC (G-CFC, GM-CFC, BFU-E or Emix-CFC) or primitive erythroid (EryP-CFC) and immunophenotypic EMPs during the maturation of two different lines of PC13 ES cells (top) or W4 ES Cells (bottom). Values are relative to maximum value seen per 10^5 EB cells during maturation. **C.** Distribution of CFC potential, definitive or primitive as defined in B as well as Mac-CFC in day 8 EB cells in immunophenotypic EMPs versus the rest of the cells (Non-EMP). Averages and SEM of 4 experiments are shown. **D.** Potential of day 9 EB kit$^+$CD41$^+$CD16/32$^+$ cells (EMP) or the VE-cadherin positive subpopulation of the remaining cells (Non-EMP VEC+) to differentiate into B-cell progenitors after 12 days of co-culture with OP9 stromal cells. Results from a negative culture started with EMPs and a positive culture of Non-EMP VEC + are shown. P13 ES cell line was used. B-cell potential was not observed in W4 ES cell line in parallel experiments although EMPs were still present.

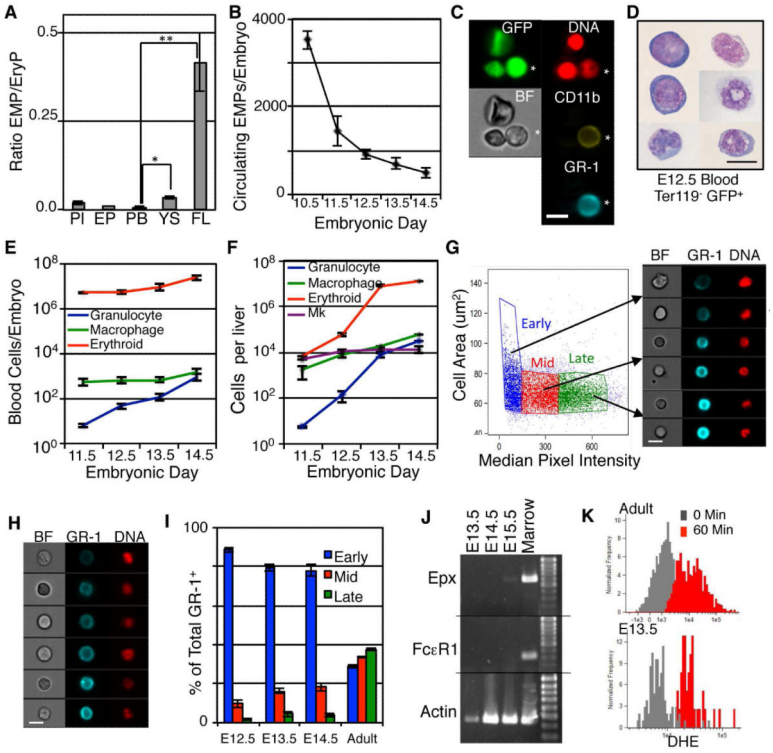

Figure 5.

EMPs migrate to the fetal liver and differentiate including generation of mature neutrophils. **A.** Enrichment of EMPs in E10.5 tissues relative to circulating primitive erythroid cells (EryP). n=3 or 4 +/− SEM. *p<0.01, **p<0.003 **B.** Numbers of circulating immunophenotypic EMPs per embryo by flow cytometry. n=3 +/− SEM. **C.** Examples of imaging flow cytometry of peripheral blood from GFP$^+$ E11.5 embryos. A nucleated primitive erythroblast is at the top of the images and the cell indicated by an asterisk is an embryonic granulocyte. Size bar=10 um **D.** Images of cytospun GFP+ Ter119-cells from E12.5 blood. Size bar =25 um **E.** Numbers of erythroid cells (Ter119$^+$), macrophages (CD11b$^+$F4/80$^+$) and granulocytes (CD11b$^+$ GR-1$^+$) per embryo in circulation. Results from 3 to 5 experiments +/− SEM. **F.** Numbers of erythroid cells, monocyte/macrophages and granulocytes per fetal liver were identified as in E. Megakaryocytes (Mk) were identified as kit$^-$ CD41$^+$ with similar light scatter values as the other cells (to eliminate platelets). Results from 3 to 5 experiments +/− SEM. **G.** Analysis of granulocytes in bone marrow divided into early, mid, and late maturational stages based on cell size and the median pixel value for GR-1. Size bar=10um **H.** Images of maturing granulocytes from E12.5 liver. Size bar=10um **I.** Proportion of granulocytes in maturational stages as in G. n=3 +/− SEM. **J.** Expression of eosinophil (eosinophil peroxidase, Epx) or basophils and mast cells (FCεR1) transcripts as determined by RT-PCR in fetal liver samples and bone marrow. **K.** Analysis of oxidative burst in adult and E13.5 peripheral blood granulocytes after simulation with bacteria-like particles. Significance of induction in fetal $p<10^{-4}$.

A

Recipient	Donor	ST	LT
i.v. C57	1000 LSK	4/4	4/4
	10000 E10.5 EMP	0/4	0/4
i.v. NSG	200 LSK	7/7	7/7
	4500 E9.5 EMP	4/5	0/5
	6000 E10.5 EMP	5/5	0/5
i.f. NSG	1000 LSK	4/7	5/7
	5300 E10.5 AGM	2/2	2/2
	7500 E10.5 EMP	4/6	0/6

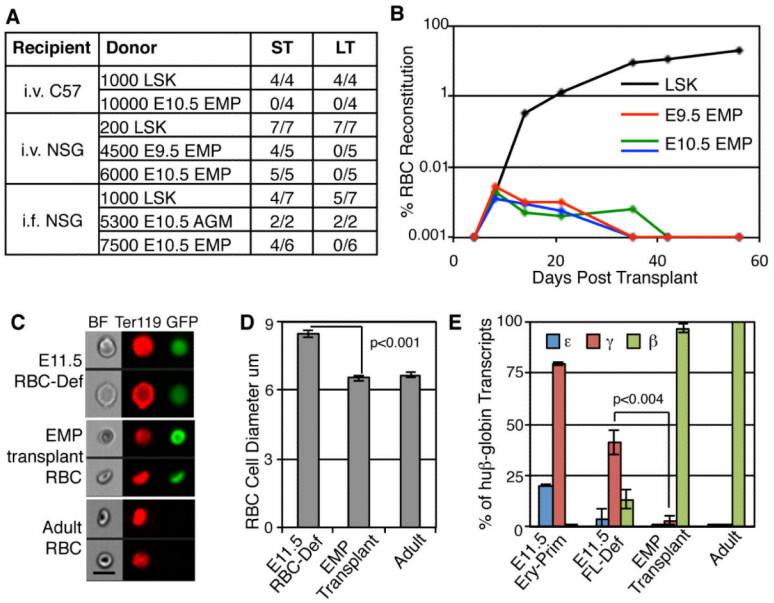

Figure 6.

EMPs engraft adult recipients and provide transient erythroid reconstitution. **A.** Frequency of mice with short-term (<8 weeks) and long-term reconstitution (>16 weeks) of blood cells after transplantation with sorted embryonic cells or bone marrow $lin^{-}kit^{+}sca^{+}$ (LSK) into wildtype or NSG recipients. **B.** Example of erythroid reconstitution after injection of 4500 E9.5 or 6000 E10.5 sorted EMPs or 200 bone marrow LSKs. **C.** Representative images of EMP-derived circulating definitive erythroid cells (E11.5 RBC-def) isolated from E11.5 blood, and EMP-derived RBCs generated in an adult recipient and as well as recipient's endogenous RBCs. Size bar=10um. **D.** Diameter of RBCs as measured by imaging flow cytometry (height of Ter119 morphology mask). Average of 3 experiments are shown +/− SEM. **E.** Expression of human beta globin genes in transgenic EMP-derived cells transplanted into non-transgenic recipients (EMP Transplant) plotted as percent of total human beta globin message detected. Expression levels from tissues in transgenic mice are shown for comparison: primitive erythroblasts from peripheral blood (E11.5 Ery-Prim), EMP-derived erythroid cells sorted from E11.5 livers (E11.5 FL-Def) to remove circulating primitive erythrocytes (McGrath et al., 2011) as well as adult RBCs. Average of 3 samples +/− SEM is shown.